Evidence for Nucleation-Growth, Redistribution, and Dissolution Mechanisms during the Course of Redox Cycling Experiments on the C_{60}/NBu_4C_{60} Solid-State Redox System: Voltammetric, SEM, and in Situ AFM Studies

Marco F. Suárez, Frank Marken, and Richard G. Compton

Physical and Theoretical Chemistry Laboratory, Oxford University, South Parks Road, OX1 3QZ Oxford, U.K.

Alan M. Bond,* Wujian Miao, and Colin L. Raston

Department of Chemistry, Monash University, Clayton, Victoria 3168, Australia

Received: March 17, 1999; In Final Form: April 13, 1999

The electrochemical reduction of solid C_{60} abrasively attached in the form of microcrystals to graphite and glassy carbon electrode surfaces and then immersed in acetonitrile containing 0.1 M NBu_4PF_6 or NBu_4ClO_4 as the electrolyte has been studied. Voltammetric responses observed after the initial stages of redox cycling experiments, when redistribution processes occur, are consistent with those observed previously for so-called "film" deposits. The characteristic "steady-state" shape of the solid-state voltammetric response with a large potential gap between reduction and reoxidation responses is shown by chronoamperometric experiments to be associated with the presence of a nucleation and growth-type mechanism. The initial three reduction processes of C_{60} attached to the electrode surface, which lead to the chemically reversible formation of only slightly soluble C_{60}^- and C_{60}^{2-} and finally to the loss of the soluble C_{60}^{3-} have been followed by ex situ SEM and in situ AFM experiments. The extent of the electrochemical conversion is shown to depend strongly on the crystal size, with larger crystals being affected only at the solid−liquid interfacial region. Evidence for stochastic processes further supports the proposed nucleation and growth-type mechanism. Crystal redistribution processes also are identified by the AFM measurements.

Introduction

There has been considerable interest in electrochemical processes which allow the direct conversion of one form of a solid material into another reduced or oxidized form, especially for the case of Buckminster-fullerene,[1] C_{60}. The driving force for these experimental studies has arisen mainly from the need for new technology for specialized energy storage devices, interest in new superconducting materials,[2] and the fundamental study of the energetics and kinetics of processes at phase boundaries in contact with an electrode.[3] The reduction of C_{60} occurs in solution[4−7] as well as in the solid state[8−15] via several consecutive one-electron steps. In the latter case, the charge neutrality for the solid-state process has been shown to be maintained by the reversible insertion of countercations such as NBu_4^+, Li^+, Cs^+, etc., from the contacting solution phase.[16,17] A recent review covers many of the advances and problems reported in this field.[18]

The electrochemical redox-cycling of solid C_{60} has been reported under a wide range of experimental conditions which include various deposition procedures such as solvent casting,[8−15] gas phase,[19] and electrochemical deposition,[20] and a range of contacting solvent systems and electrolyte salts. The interaction of the solid with neutral solution species[21,22] and also catalytic processes[23] have been noted. Most extensive work has been published on the redox-cycling of solid C_{60} deposited on an electrode and immersed in an acetonitrile solution containing NBu_4^+ cations. For this system, the starting material, C_{60}, as well as the products from the first two reduction steps are sufficiently insoluble for the process to be dominated by a solid−solid pathway since the loss of material from the electrode into the solution phase is small. In the complex reaction scheme,[18] the dissolution of C_{60}^- and the solid-state conversion are proposed to occur as parallel processes. However, mechanistic details related to the solid-state process are not well understood and phenomena due to "film" porosity and potential-dependent changes of conductivity[24] further complicate the system.

The reduction of C_{60} deposits has been shown to involve factors such as counter-ion (cation) uptake and transport into the deposit, significant structural rearrangements on reduction and reoxidation, resistivity changes, and dissolution[18,20,21] on the basis of EQCM and elegant SECM[8,9] studies. On the basis of mass spectrometry studies, Zhou et al.[25] have suggested that the NBu_4^+ cations are likely to be partially retained in the deposit under certain conditions.

In contrast to previous studies in which thin "films" of material of differing density have been applied to electrode surfaces, the work described in this study focuses on the *direct* use of microcrystalline C_{60}. For films of C_{60}, cracks and imperfections may be the key factors in allowing electrochemical processes to occur. Experimental evidence for high porosity of C_{60} deposits formed by solvent casting comes most evidently from SECM[9] and hydrodynamic voltammetry.[16,24] The direct use of microcrystalline solid is therefore a very suitable approach for mechanistic characterization of the process because it eliminates the possibility of complications due to the presence of entrapped solvent molecules. The direct use of solid C_{60}

* Correspondong author: Telephone: (61)(3) 9905 1338. Fax: (61)(3) 9905 4597. E-mail: a.bond@sci.monash.edu.au.

10.1021/jp990926x CCC: $18.00
Published on Web 06/19/1999

mixed into a poly-ethylene oxide matrix has been reported by Chabre et al.[26] In the present study, the reduction of microcrystalline C_{60} abrasively attached to suitable electrode surfaces is shown via electrochemical experiments and other data to proceed via a nucleation and growth type mechanism. Ex situ SEM and in situ AFM images of the process are presented to confirm the presence of this mechanism which also is believed to be relevant to previous studies with "films".

Experimental Section

Reagents. Solvents used were acetonitrile (dried and distilled, Fisons), dichloromethane, and toluene (both HPLC grade, Aldrich). Electrochemical grade tetrabutylammonium perchlorate, NBu_4ClO_4, Fluka, or tetrabutylammonium hexafluorophosphate, NBu_4PF_6, Fluka, supporting electrolyte and C_{60} (>99.9%, MER Corporation, U.S.A.) were used as received. Solutions were thoroughly degassed with Pureshield argon (BOC) for at least 15 min prior to experiments.

Instrumentation. For electrochemical experiments either a Cypress Systems Model CS-1090 computer-controlled electroanalytical system, an Autolab PGSTAT 20 System (Eco Chemie, Netherlands), or an Oxford Electrodes Bipotentiostat controlled via a Topometrix AFM system were employed. Electrodes used were a 4.9 mm diameter basal plane pyrolytic graphite disk (Pyrocarbon, Le Carbone Ltd., Sussex, U.K.) mounted in Teflon, a 3 mm diameter glassy carbon disk (BAS Technicol Ltd., Cheshire, U.K.), or a 3 mm diameter platinum disk. A platinum wire served as the counter electrode and the reference electrode was a saturated calomel electrode (SCE) (with $E_{1/2,\text{ferrocene}} = 0.38$ V vs SCE) in conventional voltammetry and a Ag/AgCl pseudo reference (with $E_{1/2,\text{ferrocene}} = 0.38$ V vs Ag/AgCl) in in situ AFM studies. For scanning electron microscopy (SEM) a JSM-840 instrument with 25 kV accelerating voltage was used. Samples were gold coated in a Balzers sputter coating unit prior to microscopy.

For in situ electrochemical atomic force microscopy (AFM) a Topometrix TMX 2010 Discoverer atomic force microscope, operating in the contact mode, was employed. Electrochemical experiments with C_{60} abrasively attached to a glassy carbon electrode were performed in a special cell supplied by Topometrix. The experimental details for the electrochemical AFM cell have been described previously.[27] Pyramidal silicon nitride tips (Topometrix AFM E-Chem probes 1750) were employed. The images were obtained with a resolution of 300×300 data points per image and the scanning rate was about 5−10 Hz. All AFM and voltammetric measurements were made under ambient temperature conditions of 20 ± 2 °C. To keep the solution phase inside the electrochemical AFM cell free of oxygen and to minimize the contamination with oxygen diffusing through the latex membrane, freshly degassed solution was flowed through the cell before and after each potential cycle experiment.

Methods described in the literature were employed[9,16,28] to characterize the morphological differences between C_{60} films prepared by solvent casting and by abrasive attachment of microcrystalline C_{60}. For the solvent evaporation deposition of C_{60} on glassy carbon and platinum the electrode surface was polished and then coated with 5−10 μL of a solution of 0.01 M C_{60} in toluene or a saturated solution (0.36 mM) of C_{60} in dichloromethane. The procedure for abrasive attachment of C_{60} consisted of spreading 2−5 mg of the solid onto a filter paper (Whatman 1) and gently rubbing the electrode surface onto it. Glassy carbon electrodes were chosen for the in situ AFM experiments because of better adhesion of the C_{60} microcrystals compared to platinum or gold electrodes. Before use, the glassy carbon electrode was polished with a succession of diamond lapping compounds (Kemet International Ltd., Kent, U.K.) from 1 μm down to 0.1 μm particle size and then sonicated for 20 min.

During a typical experiment, an electrode area of between 1×1 and 50×50 μm^2 was initially imaged at open circuit potential. Subsequently a potential of 0.0 V vs Ag/AgCl was applied to the C_{60} modified glassy carbon electrode and then the topographic changes occurring during about 300 s were recorded. Finally, topographic images at different locations on the electrode surface were obtained after cycling the potential over the range between 0.0 V and −1.0 V, −1.2 V, or −1.6 V vs Ag/AgCl. The potential scan rate used in all voltammetric experiments was 0.1 V s^{-1}.

Results and Discussion

Preparation of C_{60} Deposits for Electrochemical Studies. Many applications and properties of thin films or deposits in electrochemistry depend strongly on their morphological (grain shape, contact between grains and the electrode) and structural (defects) properties. Surprisingly, relatively little is known about the morphology and the structure of the C_{60} deposits employed in earlier voltammetric studies, despite the fact that a range of techniques such as SEM, mass spectrometry, and quartz crystal microbalance have been applied in conjunction with the electrochemical measurements. Presumably, because of experimental simplicity, the deposition of C_{60} at the electrode surface by solvent evaporation has been by far the most widely used technique in electrochemical studies.[9−16] The most commonly used solvents for this purpose have been[18] benzene, dichloromethane, and toluene. Differences in the morphology and porosity of the deposits may be expected due to the rate of nucleation and crystallization, which are related to the rate of solvent evaporation, the solution concentration, and the roughness of the electrode surface. These factors together with the deposition procedure are believed to influence the morphology, topography, and the mechanical stability of the resulting deposit.

In Figure 1, a comparison of AFM images of C_{60} deposits prepared by different protocols is shown. Figure 1a shows the typical morphology of the C_{60} microcrystals formed on a glassy carbon electrode by evaporation of 5 μL of 0.01 M C_{60} in toluene solution. It can clearly be seen that the deposit does not completely cover the substrate surface and it is composed of various differently shaped single crystals and starlike agglomerates. This morphology is similar to that reported for a very nonuniform C_{60} deposit grown by a sublimation procedure.[29,30]

Nanometer scale microcrystals and a much more uniform thin layer of C_{60} were formed on glassy carbon surfaces by evaporation of 10 μL of a saturated solution of C_{60} in dichloromethane solution (Figure 1b). The fact that the deposits formed from an organic solvent of relatively low boiling point such as dichloromethane are more homogeneous may account for the better reproducibility of the electrochemical behavior of these deposits described in earlier reports.[10,16]

Finally, the abrasive attachment of crystalline C_{60} to a glassy carbon electrode surface (Figure 1c) results in a deposit characterized by both areas of low coverage with very small particles and areas of high coverage with conglomerates of particles.

Voltammetry of Solid C_{60} Mechanically Attached to a Graphite Electrode. A marked difference is usually observed between the first and subsequent scans during potential cycling

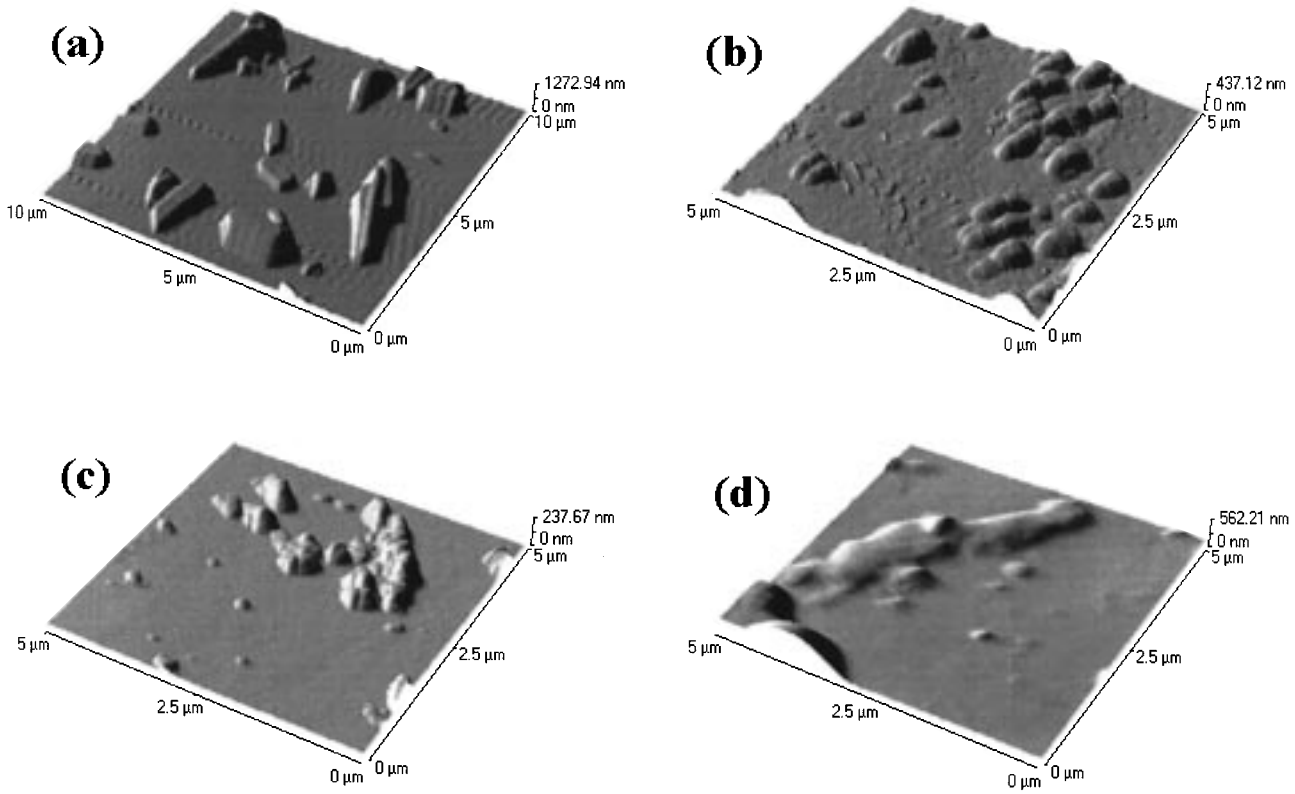

Figure 1. (a) and (b) are AFM images obtained in air of microcrystals of C_{60} formed on glassy carbon (a) by evaporation of a 5 μL solution of 0.01 M C_{60} in toluene, and (b) by evaporation of a 10 μL saturated solution of C_{60} in dichloromethane. In (c), an AFM image of a glassy carbon electrode surface modified by mechanically adhered C_{60} is shown after immersion in acetonitrile/0.1 M NBu_4ClO_4, and in (d) the effect of cycling the electrode potential over 10 cycles (scan rate 0.1 V s^{-1}) between 0 and -1.0 V vs Ag/AgCl is shown.

voltammetric experiments with drop-coated films[10,16] and with vapor-deposited C_{60} film,[31] irrespective of whether only the first or the first two reduction processes were studied. The first two reductions were proposed to overlap during the first voltammetric scan recorded for a relatively thick C_{60} deposit[16] but became resolved on subsequent scans. Similar behavior was observed by Nishizawa et al.[31] for compact vapor-deposited films and by Koh et al.[32] for electrochemically grown films. These reports suggest that the preparation method and the initial film structure affect the initial electrochemical behavior of the film. Nishizawa[31] suggested that the initial reduction needs an overpotential for the incorporation of the cation into the C_{60} structure and this initial activation process may facilitate the redox reaction in the subsequent potential sweeps. However, it has also been noted[18] that for the electro-insertion of NBu_4^+ cations, independent of the deposition procedure used, voltammetric responses become very similar after about 10 initial potential cycles when a "steady state" is reached.

In Figure 2, cyclic voltammograms obtained for solid C_{60} mechanically attached to a basal plane pyrolytic graphite electrode are shown. In the initial 10 potential cycles between 0.0 and -1.0 V vs SCE (not shown), a somewhat broad reduction signal develops into the relatively stable "steady-state" voltammetric response which is characteristic for the C_{60}/NBu_4C_{60} system.[32] The first redox couple labeled A^{red} and A^{ox} in Figure 2a has been shown[33] to correspond to a one-electron reduction process (eq 1).

$$[C_{60}]_{solid} + e^- + NBu_4^+ \rightarrow [C_{60}NBu_4]_{solid} \quad (1)$$

The scans shown in Figures 2b and 2c also contain, respectively, the second and third one-electron redox conversions labeled B^{red}, B^{ox}, and C^{red} (eqs 2 and 3).

$$[C_{60}NBu_4]_{solid} + e^- + NBu_4^+ \rightarrow [C_{60}(NBu_4)_2]_{solid} \quad (2)$$

$$[C_{60}(NBu_4)_2]_{solid} + e^- \rightarrow [C_{60}^{3-}]_{solution} + 2\ NBu_4^+ \quad (3)$$

The characteristic features and the complexity of the observed voltammetric responses obtained for the reduction of microcrystals of solid C_{60} attached to basal plane pyrolytic graphite electrodes after repetitive cycling of the potential, appear to be very similar to those described previously. This result and the AFM images shown in Figure 1 suggest that processes which have been attributed in previous studies to "films" are probably more accurately described as processes associated with reactions of arrays of solid particles or crystalline deposits.

The voltammetric data observed for the reduction of solid C_{60} abrasively attached to basal plane pyrolytic graphite or glassy carbon electrode are summarized in Table 1 and compared to data obtained for the reduction of C_{60} deposited by dichloromethane evaporation onto a platinum electrode.[16] The reduction and reoxidation current responses can be identified unequivocally. The peak width at half-height of the voltammetric responses is in most cases small compared to the peak width of 91 mV expected theoretically[34] for a "thin film" of noninteracting redox centers. The peak potentials, especially for the first chemically reversible reduction redox couple, $A^{red} - A^{ox}$, can be seen to exhibit a wide separation or "inert zone" of $\Delta E_p^{ox-red} = 0.52$ V which is characteristic for a wide range of solid-state electrochemical processes. This behavior has been attributed to structural changes associated with the process of cation insertion and expulsion into/from the solid or other mechanisms. Recently, systems with large peak separations have been interpreted in terms of a nucleation and growth mechanism.[35] For example, with the closely related cases of reduction of solid 7,7,8,8-tetracyanoquinodimethane (TCNQ)[36−38] and the

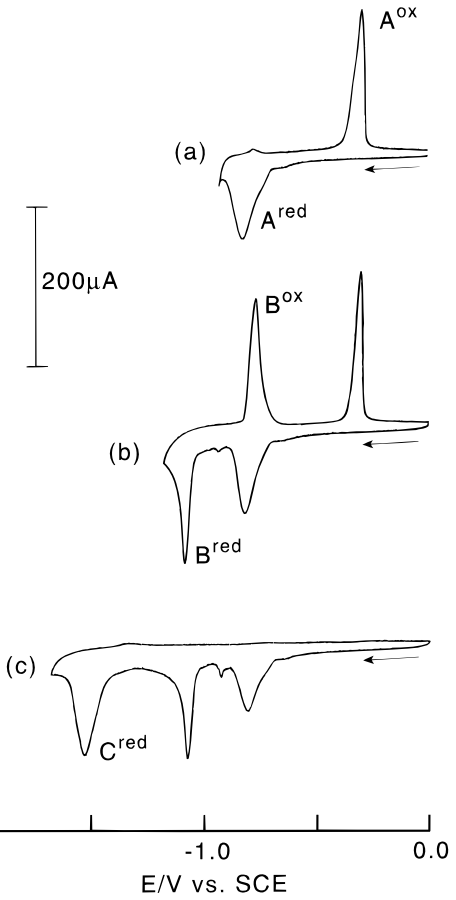

Figure 2. Cyclic voltammograms obtained for the reduction and reoxidation of solid C_{60} mechanically attached to a basal plane pyrolytic graphite electrode immersed in acetonitrile/0.1 M NBu_4PF_6. (a), (b), and (c) show the eleventh cycle of the potential and subsequent cycles with a more negative switching potential (scan rate 0.02 V s^{-1}, $T = 20 \pm 2$ °C).

TABLE 1: Voltammetric Data for the Reduction of Solid C_{60}[a]

	E_p/V vs SCE			ΔE_p^{ox-red}/mV			peak width $\Delta E_{p,1/2}$/mV		
peak	(a)	(b)	(c)	(a)	(b)	(c)	(a)	(b)	(c)
A^{red}	−0.82	−0.80	−0.83				100	70	85
A^{ox}	−0.30	−0.22	−0.28	520	580	550	58	70	85
B^{red}	−1.08	−0.99	−0.99				47	50	45
B^{ox}	−0.77	−0.77	−0.80	310	220	190	60	50	45
C^{red}	−1.53	−1.41	−1.42				100	ca. 200	80

[a] (a) Mechanically attached to a basal plane pyrolytic graphite electrode and immersed in acetonitrile/0.1 M NBu_4PF_6, (b) Deposited by a dichloromethane evaporation method[16] onto a platinum electrode, and (c) Mechanically adhered to a glassy carbon electrode immersed in acetonitrile/0.1 M NBu_4ClO_4 (scan rate 0.1 Vs^{-1}).

oxidation of tetrathiafulvalene[39] this mechanism seems preferable to other schemes that have been reported.[40]

In the case of C_{60}, strong evidence for the presence of nucleation-growth type kinetics in the interconversion of C_{60} microcrystals is provided by chronoamperometric (double potential step) experiments. In Figure 3 the results of two successive potential step experiments are shown for the reduction of C_{60} mechanically attached to a basal plane pyrolytic graphite electrode immersed in acetonitrile/0.1 M NBu_4PF_6 after 10 redox cycling experiments had been undertaken (see above). It is clearly seen in this figure that both the reduction at $E = -0.850$ V vs SCE and the reoxidation current−time profile at $E = -0.205$ V vs SCE exhibit "rising" current transients rather

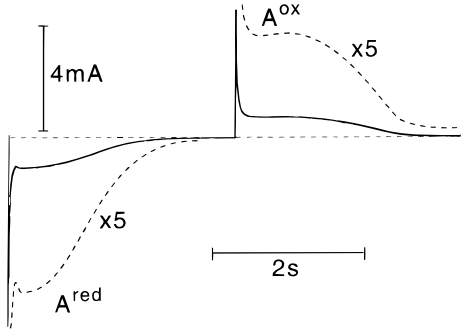

Figure 3. Chronoamperogram for the reduction and reoxidation of solid C_{60} mechanically attached to a basal plane pyrolytic graphite electrode and immersed in acetonitrile/0.1 M NBu_4PF_6. Potential steps are from 0 to −0.85 V for reduction and −0.85 to −0.205 V vs SCE for reoxidation after 10 initial potential cycles between 0 and −1.0 V vs SCE.

than the monotonic decay of the current usually observed with diffusion or electron transfer controlled systems. That is, the current−time transients include well-defined peaks. The existence of peaks in response to potential steps is highly characteristic for solid-state processes associated with nucleation-growth kinetics. With this mechanism, the slow formation of nuclei is followed by almost "explosive" growth at large overpotentials[41] which explain the large separation of peak potentials and very narrow widths at half peak height. A very interesting question concerning this process is the exact nature and location of the nuclei. Calculations show that from an energetic point of view the most likely location is at the triple interface between solid, electrode, and solution phase.[35]

Examination of C_{60} and NBu_4C_{60} Solids by the ex Situ SEM Technique. A study reporting the morphological changes which occur upon reduction of a film of C_{60} vapor deposited onto a platinum electrode and immersed in 0.1 M NBu_4PF_6 in acetonitrile has led to the conclusion that crystalline products may be obtained upon reduction to a NBu_4C_{60} film.[19] In agreement with mass spectroscopy and EQCM[20,25] evidence, results implied that these crystalline reduced products can be formed irreversibly. It has also been reported that the extent of formation of the microcrystals depends on the film thickness, with the thicker films resulting in a higher coverage of crystals.[19]

In Figure 4, SEM images are shown for C_{60} deposited by CH_2Cl_2 evaporation onto a basal plane pyrolytic graphite electrode before and after electrochemical reduction at $E = -1.0$ V vs SCE. In agreement with the AFM images shown in Figure 1b, the dichloromethane evaporation method leaves behind an array of solid, almost shapeless, particles deposited on the basal plane pyrolytic graphite rather than a film. After electrochemical reduction of the deposit at $E = -1.0$ V vs SCE for 60 s in acetonitrile/0.1 M NBu_4PF_6, removal from the solution, air-drying, and sputter coating, the morphology of the deposit has clearly changed and a crystalline product identified as NBu_4C_{60} has been formed (Figure 4b). This morphology change requires considerable mass transport and it can be seen that some of the initial C_{60} material does not appear to have been converted to the well-defined microcrystalline form. However, although the crystalline product observed after reduction resembles that observed by Tomura et al.,[19] data obtained by ex situ experiments in the absence of the solvent (electrolyte) phase have to be treated with care.

Examination of Redox Cycling Experiments of Solid C_{60} by in Situ AFM. The study of processes involving the formation or dissolution of solid materials at electrode/solution interfaces

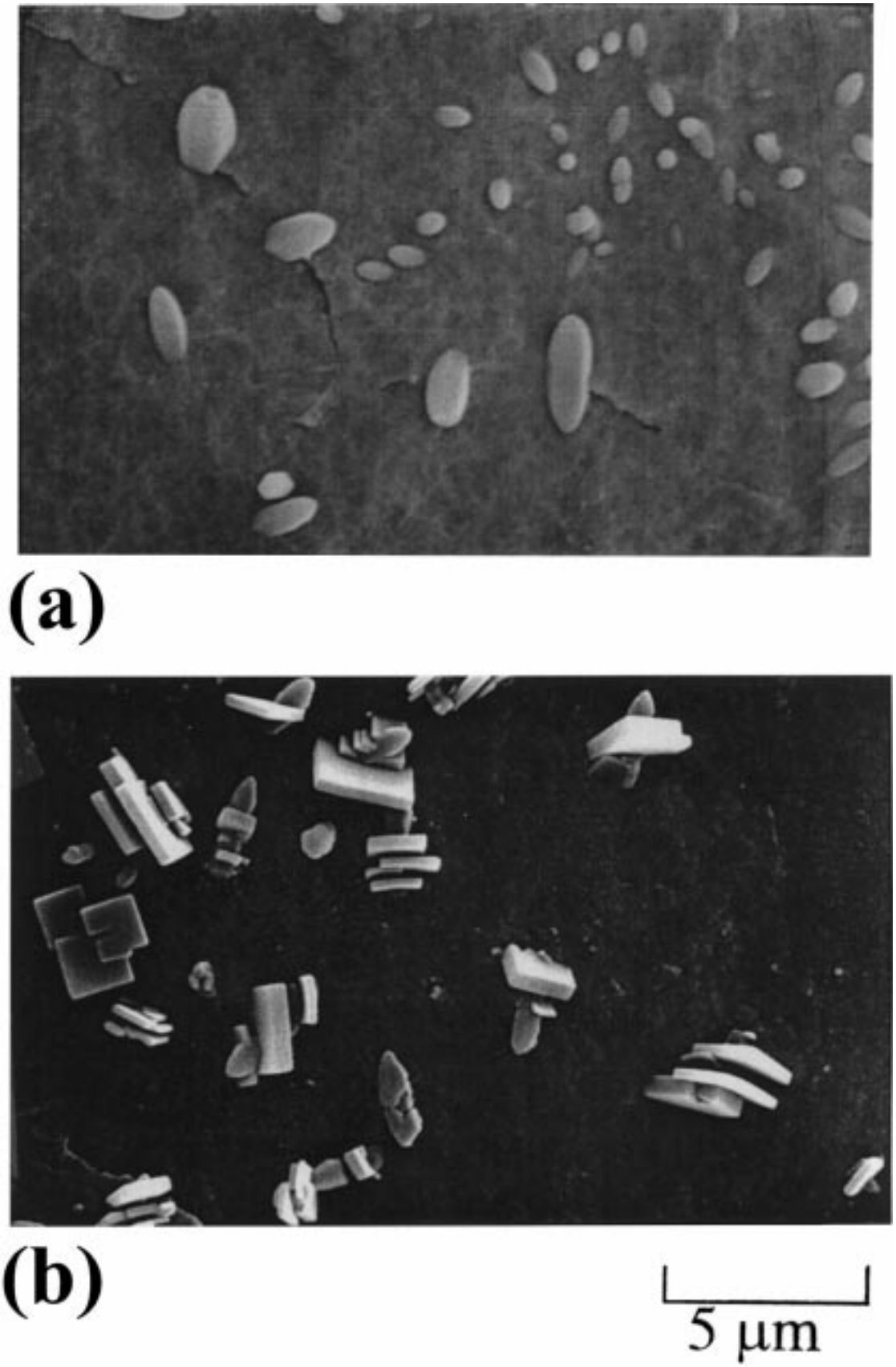

Figure 4. SEM images obtained for C_{60} deposited onto a basal plane pyrolytic graphite electrode by solvent evaporation of a saturated solution of C_{60} in dichloromethane: (a) before and (b) after a period of 60 s reduction at −1.0 V vs SCE in acetonitrile/0.1 M NBu_4PF_6.

by in situ AFM techniques has been developed and applied successfully in recent years.[42] However, even though problems with less rigidly attached solids as formed in this work may arise, it has been shown that the electrochemical solid−solid conversion of mechanically attached solids, e.g., TCNQ, can be monitored directly by in situ AFM.[43]

Figure 1c shows a typical AFM image of solid C_{60} abrasively attached to a glassy carbon electrode. The original C_{60} material

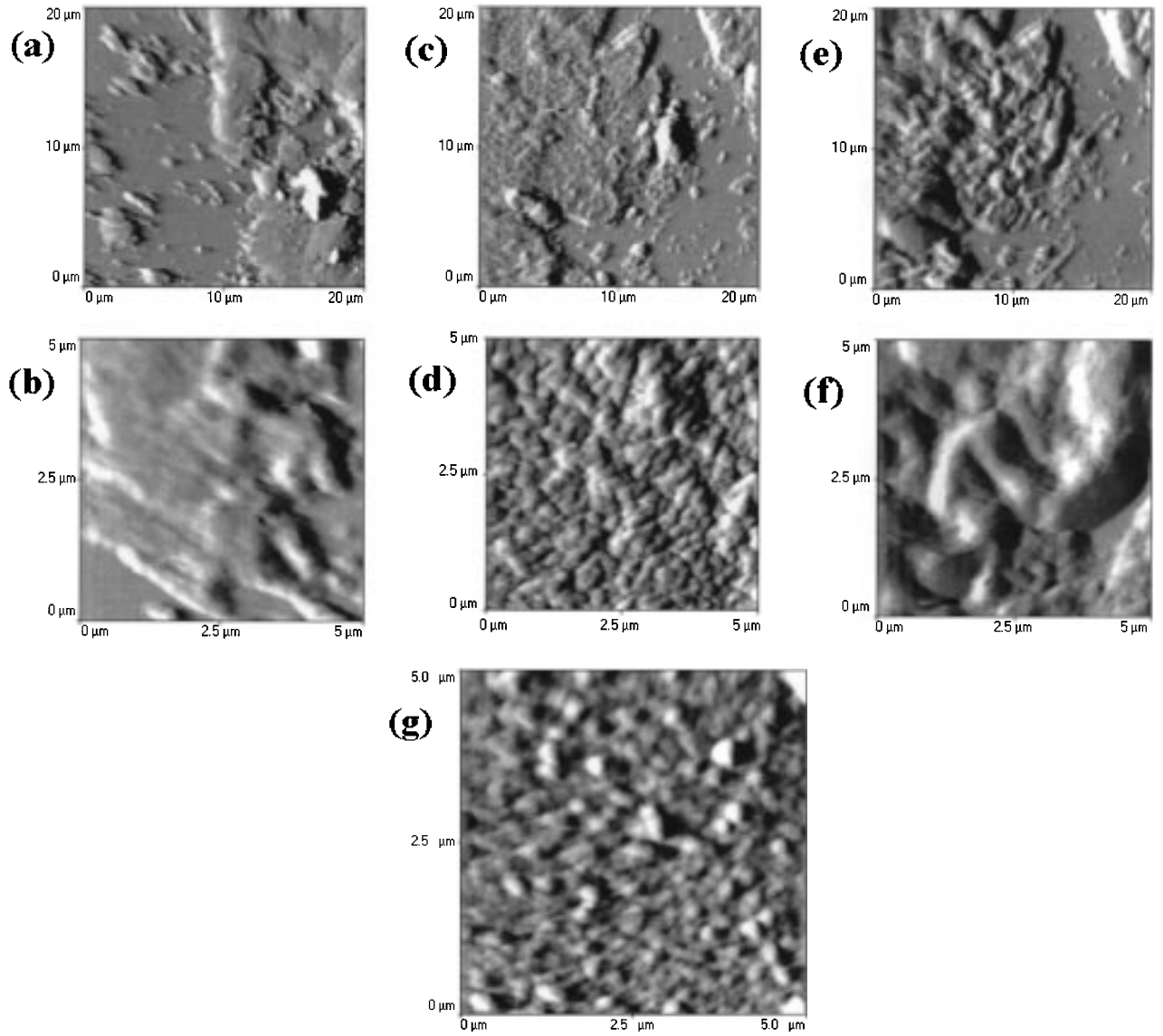

Figure 5. In situ AFM images obtained at 0 V in acetonitrile/0.1 M NBu_4ClO_4 showing the changes in the morphology that occur when C_{60} mechanically adhered as a crystalline solid to a glassy carbon electrode is subjected to redox cycling experiments (scan rate 0.1 V s^{-1}). C_{60} microcrystals after (a,b) 10 potential cycles between 0 and −1.0 V, (c,d) after 2 further cycles between 0 and −1.2 V, (e,f) after 8 further cycles between 0 and −1.2 V, (g) after 3 additional cycles between 0 and −1.6 V vs Ag/AgCl. Scale: (a) 1.5 μm, (b) 0.9 μm, (c) 2.2 μm, (d) 0.6 μm, (e) 3.0 μm, (f) 1.4 μm, and (g) 0.2 μm.

adhered by abrasive attachment can be seen to be composed mainly of small particles between 200 and 300 nm in size. These combined with larger-sized single particles and micron-scale conglomerates of C_{60} particles give rise to areas of low and high coverage. Consequently, monitoring the topography changes that occur as the potential was scanned proved to be difficult because of the time it takes to record a good quality image over a wide area of surface and probably also because of formation of mechanically sensitive reduction products. Therefore, the monitoring of morphology changes was undertaken after redox cycling experiments for a specified number of cycles. Figures 1d and 5a,b show typical images at different levels of magnitude of the same electrode surface at 0.0 V after 10 redox cycles between 0.0 and −1.0 V have been applied, which reveal that the surface of the larger conglomerates becomes smoother and the smaller particles spread and lose their sharp boundaries. The extent of conversion of C_{60} to NBu_4C_{60} solids and vice versa during the course of each redox cycle is not known in detail but it is very likely that especially for the larger conglomerates only partial conversion is achieved. However, even for these larger conglomerates it is interesting to note that the surface appears to be affected by the change in topography which indicates that probably a surface-based process occurs leaving a considerable amount of original C_{60} material "buried" under the "active" layer.

During the course of the redox cycling experiments between 0 and −1.2 V, which take place with a switching potential that corresponds to the case of the first two reduction steps, further substantial changes in topography were observed. Figure 5c−f shows a sequence of images of a typical part of the glassy carbon surface containing adhered C_{60} after 10 cycles between 0 and −1 V, and 2 cycles between 0 and −1.2 V (Figure 5c,d) and 10 cycles between 0 and −1.2 V vs Ag/AgCl (Figure 5e,f). The five micron-scale images of the surface of the conglomerates reveal that the roughness increases with the number of redox cycles, and considerable redistribution of material is evident on the electrode surface. On the other hand, in areas of low coverage (not shown), no significant change in topography is

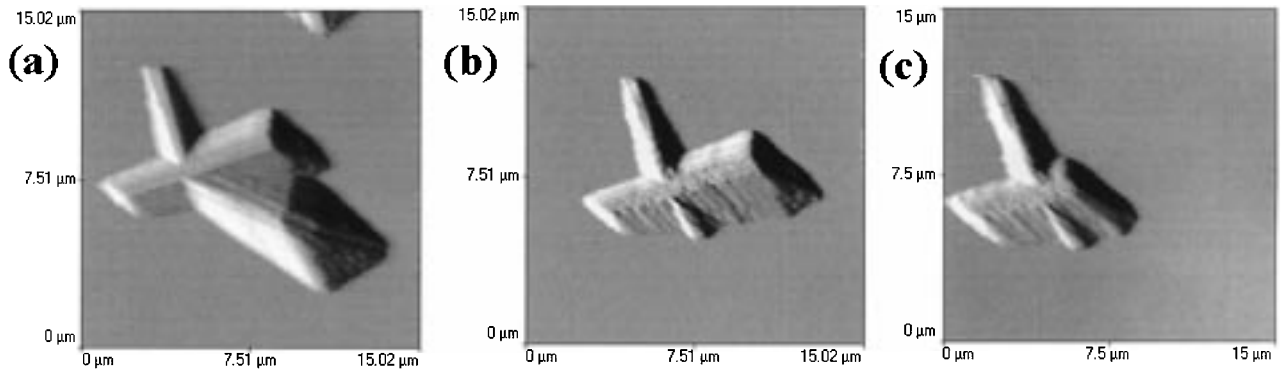

Figure 6. Morphology changes in C_{60} microcrystals deposited on a glassy carbon electrode by evaporation of a 5 μL solution of 0.01 M C_{60} in toluene during the course of redox cycling experiments between 0 and −1.0 V vs Ag/AgCl: (a) fresh deposit, (b) after one potential cycle, and (c) after four potential cycles in acetonitrile/0.1 M NBu_4ClO_4 (scan rate 0.1 V s^{-1}).

observed. This suggests that the redistribution of material occurs to achieve a lower energy configuration after addition of two electrons.

Finally, by redox cycling over a potential range that encompasses the third reduction−oxidation step (between 0 to −1.6 V vs Ag/AgCl) most of the material was lost from the surface of the electrode during only one cycle. This conclusion is reached by inferring that the height of material observed in Figure 5g, 0.2 μm, is only a fraction of that observed in previously described experiments, typically 1−3 μm. Interestingly, a very thin film of material remained on the electrode surface even after the voltammetric activity was lost. It seems that the loss of activity is due not only to the dissolution of C_{60} as it has been suggested by Tatsuma[44] but also to the formation of a film of non electrochemically active material. Jehoulet et al.[9] also reported the presence of a resistive film on the electrode surface after C_{60} lost its electrochemical activity.

To compare the above results with the morphology changes of the C_{60} deposits formed by the solvent casting process, the topography changes of C_{60} microcrystals formed by toluene solution evaporation on a glassy carbon electrode surface was studied. Figure 6 shows a sequence of topography changes of a crystal conglomerate before, after one, and after four redox cycles between 0 and −1 V. It can clearly be seen that the microcrystals become smaller with each redox cycling and the roughness of the surface of the microcrystals simultaneously increases suggesting the occurrence of a surface reaction. A notable feature observed in this topography sequence (Figure 6) for the first reduction process of C_{60} crystals is the apparent nonuniform reactivity of the crystal deposit. Areas of low and high reactivity can be identified, and the presence of stochastic nucleation-growth type kinetics may be responsible for this pattern.

Conclusions

The present studies show that the longer time scale processes involved in the electrochemical reduction and reoxidation of solid C_{60} mechanically attached to electrode surfaces closely resemble those observed for deposits formed by solvent evaporation or gas-phase deposition. That is, after a few initial cycles of the potential the same voltammetric features are observed irrespective of the method of the material deposition. Importantly, evidence for a nucleation−growth type mechanism has been obtained and is supported by SEM and AFM images. However, a quantitative model of the complex processes involved in electrochemical solid−solid conversion processes such as those observed for the C_{60}/NBu_4C_{60} system has yet to evolve, but it does appear that models that assume the presence of a "film" of material are inappropriate.

Acknowledgment. We thank COLCIENCIAS for a studentship for M.F.S. F.M. gratefully acknowledges The Royal Society for a University Research Fellowship and New College (Oxford) for a Stipendiary Lectureship. A.M.B. expresses his appreciation to Oxford University for their generous hospitality shown during his period of leave from Monash University as the 1998 Hinshelwood Lecturer during which time the majority of the University Collaborative Studies described in this paper were undertaken. Denise Fernando (La Trobe University, Melbourne) and Christiaan H. Goeting (Oxford University) are acknowledged for assistance with SEM measurements.

References and Notes

(1) See, for example, *Recent Advances in the Chemistry and Physics of Fullerenes and related Materials*; Kadish, K. M., Rouff, R. S., Eds.; The Electrochemical Society: Pennington NJ, 1994.
(2) See, for example, Liu, X. H.; Wan, W. C.; Owens, S. M.; Broderick, W. E. *J. Am. Chem. Soc.* **1994**, *116*, 5489.
(3) See, for example, Scholz, F.; Meyer, B. *Electroanal. Chem.* **1998**, *20*, 1.
(4) Dubois, D.; Kadish, K. M.; Flanagan, S.; Wilson, L. J. *J. Am. Chem. Soc.* **1991**, *113*, 7773.
(5) Xie, Q. S.; Perez-Cordero, E.; Echegoyen, L. *J. Am. Chem. Soc.* **1992**, *114*, 3978.
(6) Ohsawa, Y.; Saji, T. *J. Chem. Soc., Chem. Commun.* **1992**, 781.
(7) Dubois, D.; Kadish, K. M.; Flanagan, S.; Haufler, R. E.; Chibante, L. P. F.; Wilson, L. J. *J. Am. Chem. Soc.* **1991**, *113*, 4364.
(8) Jehoulet, C.; Bard, A. J.; Wudl, F. *J. Am. Chem. Soc.* **1991**, *113*, 5456.
(9) Jehoulet, C.; Obeng, Y. S.; Kim, Y. T.; Zhou, F. M.; Bard, A. J. *J. Am. Chem. Soc.* **1992**, *114*, 4237.
(10) Compton, R. G.; Spackman, R. A.; Wellington, R. G.; Green, M. L. H.; Turner, J. *J. Electroanal. Chem.* **1992**, *327*, 337.
(11) Szücs, A.; Tolgyesi, M.; Csiszar, M.; Nagy, J. B.; Novak, M. *J. Electroanal. Chem.* **1998**, *442*, 59.
(12) Szücs, A.; Tolgyesi, M.; Szücs, E.; Nagy, J. B.; Novak, M. *J. Electroanal. Chem.* **1997**, *429*, 27.
(13) Szücs, A.; Tolgyesi, M.; Novak, M.; Nagy, J. B.; Lamberts, L. *J. Electroanal. Chem.* **1996**, *419*, 39.
(14) Szücs, A.; Loix, A.; Nagy, J. B.; Lamberts, L. *Synth. Met.* **1996**, *77*, 227.
(15) Szücs, A.; Loix, A.; Nagy, J. B.; Lamberts, L. *J. Electroanal. Chem.* **1996**, *402*, 137.
(16) Compton, R. G.; Spackman, R. A.; Riley, D. J.; Wellington, R. G.; Eklund, J. C.; Fisher, A. C.; Green, M. L. H.; Doothwaite, R. E.; Stephens, A. H. H.; Turner, J. *J. Electroanal. Chem.* **1993**, *344*, 235.
(17) Balch, A. C.; Costa, D. A.; Fawcett, W. R.; Winkler, K. *J. Electroanal. Chem.* **1997**, *427*, 137.
(18) Chlistunoff, J.; Cliffel, D.; Bard, A. J. *Thin Solid Films* **1995**, *257*, 166.
(19) Tomura, K.; Nishizawa, M.; Takemura, D.; Matsue, T.; Uchida, I. *Chem. Lett.* **1994**, 1365.
(20) Koh, W. Y.; Dubois, D.; Kutner, W.; Jones, M. T.; Kadish, K. M. *J. Phys. Chem.* **1993**, *97*, 6871.

(21) Cliffel, D. E.; Bard, A. J.; Shinkai, S. *Anal. Chem.* **1998**, *70*, 4146.
(22) Carlisle, J. J.; Wijayawardhana, C. A.; Evans, T. A.; Melaragno, P. R.; Ailin-Pyzik, I. B. *J. Phys. Chem.* **1996**, *100*, 15532.
(23) D'Souza, F.; Choi, J.; Hsieh, Y. Y.; Shriver, K.; Kutner, W. *J. Phys. Chem. B* **1998**, *102*, 212.
(24) Szücs, A.; Tölgyesi, M.; Csiszar, M.; Nagy, J. B.; Novak, M. *Electrochim. Acta* **1998**, *44*, 613.
(25) Zhou, F. M.; Yau, S. L.; Jehoulet, C.; Laude, D. A.; Guan, Z. Q.; Bard, A. J. *J. Phys. Chem.* **1992**, *96*, 4160.
(26) Chabre, Y.; Djurado, D.; Armand, M.; Ramanow, W. R.; Coustel, N.; McCauley, J. P.; Fischer, J. E.; Smith, A. B. *J. Am. Chem. Soc.* **1992**, *114*, 764.
(27) Suarez, M. F.; Compton, R. G. *J. Electroanal. Chem.* **1999**, *462*, 211.
(28) Bond, A. M.; Colton, R.; Daniels, F.; Fernando, D. R.; Marken, F.; Nagaosa, Y.; Van Steveninck, R. F. M.; Walter, J. N. *J. Am. Chem. Soc.* **1993**, *115*, 9556.
(29) Atamny, F.; Baiker, A.; Muhr, H. J.; Nesper, R. *Fresenius' J. Anal. Chem.* **1995**, *353*, 433.
(30) Krätschmer, W. *Nanostruct. Mater.* **1995**, *6*, 65.
(31) Nishizawa, M.; Matsue, T.; Uchida, I. *J. Electroanal. Chem.* **1993**, *353*, 329.
(32) The initial potential cycles involve more complex processes affecting the first (A^{red}) and especially the second (B^{red}) reduction signal. The exact nature of these processes which are probably related to "breaking-in" or "redistribution" is not well-known.
(33) Koh, W.; Dubois, D.; Kutner, W.; Jones, M. T.; Kadish, K. M. *J. Phys. Chem.* **1992**, *96*, 4163.
(34) Hubbard, A. T.; Anson, F. C. *Electroanal. Chem.* **1970**, *4*, 129.
(35) Bond, A. M.; Fletcher, S.; Marken, F.; Shaw, S. J.; Symons, P. G. *J. Chem. Soc., Faraday Trans.* **1996**, *92*, 3925.
(36) Bond, A. M.; Fletcher, S.; Symons, P. G. *Analyst* **1998**, *123*, 1891.
(37) Chambers, J. Q.; Scaboo, K.; Evans, C. D. *J. Electochem. Soc.* **1996**, *143*, 3039.
(38) Scaboo, K. M.; Chambers, J. M. *Electrochim. Acta* **1998**, *43*, 3257.
(39) Shaw, S. J.; Marken, F.; Bond, A. M. *Electroanalysis* **1996**, *8*, 732.
(40) Evans, C. D.; Chambers, J. Q. *Chem. Mater.* **1994**, *6*, 454.
(41) Fletcher, S.; Halliday, C. S.; Gates, D.; Westcott, M.; Lwin, T.; Nelson, G. *J. Electroanal. Chem.* **1983**, *159*, 267.
(42) Li, J.; Wang, E.; Green, M.; West, E. P. *Synth. Metals* **1995**, *74*, 127.
(43) Suarez, M. F.; Bond, A. M.; Compton, R. G. *J. Solid State Electrochem.*, in press.
(44) Tatsuma, T.; Kikuyama, S.; Oyama, N. *J. Phys. Chem.* **1993**, *97*, 12067.